

Human Monocyte Subsets at Homeostasis and Their Perturbation in Numbers and Function in Filarial Infection

Roshanak Tolouei Semnani, Vanessa Moore, Sasisekhar Bennuru, Renee McDonald-Fleming, Sundar Ganesan, Rachel Cotton, Rajamanickam Anuradha, Subash Babu, Thomas B. Nutman

Laboratory of Parasitic Diseases, National Institute of Allergy and Infectious Diseases, National Institutes of Health, Bethesda, Maryland, USA

To characterize the function and plasticity of the major human circulating monocyte populations and to explore their role in systemic helminth infection, highly purified (by flow-based sorting) human monocyte subsets (CD14^{hi}/CD16^{neg} [classical], CD14⁺ or ^{hi}/CD16^{med} [intermediate], and CD14^{neg}/CD16^{hi} [nonclassical]) were examined at homeostasis and after activation. Among these three subsets the classical and intermediate subsets were found to be the major sources of inflammatory and regulatory cytokines, as well as cytokines/chemokines associated with alternative activation, whereas the nonclassical and classical populations demonstrated an ability to transmigrate through endothelial monolayers. Moreover, it was primarily the classical subset that was the most efficient in promoting autologous T cell proliferation. The distribution of these subsets changed in the context of a systemic helminth (*Wuchereria bancrofti*) infection such that patent infection altered the frequency and distribution of these monocyte subsets with the nonclassical monocytes being expanded (almost 2-fold) in filarial infection. To understand further the filarial/monocyte interface, *in vitro* modeling demonstrated that the classical subset internalized filarial antigens more efficiently than the other two subsets but that the parasite-driven regulatory cytokine interleukin-10 was exclusively coming from the intermediate subset. Our data suggest that monocyte subsets have a differential function at homeostasis and in response to helminth parasites.

Human blood monocytes are heterogeneous and can be subdivided into at least three populations based on their expression of CD14 and CD16 (CD14^{hi}/CD16^{neg} [classical], CD14⁺ or ^{hi}/CD16^{med} [intermediate], and CD14^{neg}/CD16^{hi} [nonclassical]) (1). While the functions of these subsets have been explored over the past several years (2–5), more recent work utilizing genome-wide analyses of these three monocyte subsets has provided insights into their interrelationships, phenotypes, and functions (5–7). Differences ascribed to these monocyte subsets relate to differences in cytokine production, antigen uptake, and antigen presentation; there is, however, little consensus among the studies, most likely attributable to differences in the isolation methods used. For example, nonclassical monocytes—generally considered poor producers of inflammatory cytokines in response to lipopolysaccharide (LPS) (8)—have been shown by others to produce tumor necrosis factor alpha (TNF- α) and interleukin-1 β (IL-1 β) upon stimulation with LPS (9). Furthermore, there are relatively inconsistent data on the monocyte subset primarily responsible for production of IL-10 (7, 8, 10, 11). In addition, until recently both intermediate and nonclassical monocytes were grouped together as a homogeneous CD16⁺ population but have since been functionally separated into two distinct populations (reviewed by Wong et al. (1)).

Monocytes derived from CD34⁺ myeloid progenitor cells in the bone marrow circulate in the blood and then enter the peripheral tissues, where they mature to macrophages (9). Tissue macrophages can also be subdivided into at least three populations: M1, characterized by an inflammatory profile induced primarily during a Th1 response; M2, which have both anti-inflammatory and tissue repair functions (9), largely driven by IL-4 and/or IL-13; and finally, regulatory macrophages (Mreg) that are considered to be the primary source of innate IL-10 (12–14). Although there is increasing evidence indicating human monocytes can be polarized *in vitro* with LPS and gamma interferon (IFN- γ) into

M1, with IL-4/IL-13 into M2, or with a combination of immune complexes and Toll-like receptor (TLR) ligands into Mreg (15, 16), little is known about the ontogeny of these subsets.

While several studies have investigated the role of monocyte subsets in bacterial, viral, and parasitic infections (17, 18; reviewed in reference 1), their roles in infection with extracellular parasites (such as filariae) have not been fully elucidated. In fact, monocyte dysfunction in filarial infection is one of several mechanisms proposed to explain parasite antigen-specific T cell hyporesponsiveness seen with patent lymphatic filariasis (19). It has previously been demonstrated that monocytes from filaria-infected individuals are studded with internalized filarial antigens, have diminished expression of genes involved in antigen presentation and processing, and produce fewer proinflammatory cytokines in response to surface receptor cross-linking (19, 20).

In the present study, we examined the function of each of the monocyte subsets at steady state in healthy donors (homeostasis), when activated with LPS/IFN- γ or IL-4, and with live microfilariae (mf). Moreover, we have put these data in context by examining how the presence of filarial antigen (that defines patent filarial infection) alters the frequency and distribution of these monocyte subsets and highlighted role played by the parasite in

Received 25 April 2014 Returned for modification 6 June 2014

Accepted 4 August 2014

Published ahead of print 11 August 2014

Editor: J. H. Adams

Address correspondence to Roshanak Tolouei Semnani, rsemnani@niaid.nih.gov.

Supplemental material for this article may be found at <http://dx.doi.org/10.1128/IAI.01973-14>.

Copyright © 2014, American Society for Microbiology. All Rights Reserved.

doi:10.1128/IAI.01973-14

TABLE 1 Demographic profile of infected and uninfected individuals in a South Indian population in Tamil Nadu where microfilariae are endemic

Parameter	GM (range) ^a		P
	INF	UN	
No. of subjects	11	13	
Age (yr)	42 (23–69)	38.5 (23–67)	
Male/female ratio	7/4	6/7	
Circulating filarial antigen (IU/ml)	2,819.75 (1,057–9,352)	<32	
White blood cell count (10 ³ /ml)	9.95 (7.00–15.60)	6.91 (4.50–9.80)	
Neutrophil count (10 ³ /ml)	5.94 (4.06–11.54)	3.94 (2.42–5.99)	
Lymphocyte count 10 ³ /ml)	2.13 (1.57–3.67)	1.95 (1.17–2.85)	
Monocyte count (10 ³ /ml)	0.66 (0.51–0.99)	0.34 (0.25–0.47)	0.0002
Eosinophil count (10 ³ /ml)	0.43 (0.24–0.68)	0.25 (0.10–0.53)	0.0264
Basophil count (10 ³ /ml)	0.07 (0.04–0.10)	0.03 (0.02–0.07)	0.0044

^a UN, uninfected healthy individuals in this region; INF, filaria-infected individuals in this region. The values indicated are expressed as geometric means and range, except for age, which is expressed as the median age and range.

the induction of IL-10 by the intermediate (CD14⁺ or ^{hi}/CD16^{med}) phenotype.

MATERIALS AND METHODS

Ethics statement. The elutriated monocytes and lymphocytes from leukopacks from healthy adult donors from North America were collected under a protocol approved by the Institutional Review Board (IRB) of the Department of Transfusion Medicine, Clinical Center, National Institutes of Health (NIH; IRB 99-CC-0168).

All individuals from India were adults and examined as part of a clinical protocol approved by the IRBs of both the National Institute of Allergy and Infectious Diseases (NIAID; USA) and the National Institute for Research in Tuberculosis (India) (NCT00375583 and NCT00001230). Informed written consent was obtained from all participants.

Healthy donors. CD14⁺ peripheral blood-derived monocytes were isolated from leukopacks from healthy donors by counterflow centrifugal elutriation. The lymphocytes were washed in phosphate-buffered saline (PBS) and cryopreserved in liquid nitrogen until needed.

Filarial patient populations. Patient cells were collected in Tamil Nadu, South India, a region where *Wuchereria bancrofti*, the major causative agent of lymphatic filariasis (LF), is endemic. Cells were obtained from 24 individuals, including 11 *W. bancrofti*-infected but clinically asymptomatic patients (here referred to as filaria infected [INF]) and 13 from uninfected control subjects from the same region (UN). All INF individuals were determined to be positive by both the immunochromatographic card test (ICT) filarial antigen test and the TropBio Og4C3 enzyme-linked immunosorbent assay (ELISA), and both INF and UN individuals had not received any antifilarial treatment prior to the present study (Table 1). There were no differences between the populations with regard to age or gender. Immunologically, the INF subjects had significantly higher absolute numbers of circulating monocytes, eosinophils, and basophils (Table 1).

Live *Brugia malayi* mf and parasite antigen. Live *B. malayi* mf were collected by peritoneal lavage of infected jirds and separated from peritoneal cells by Ficoll diatrizoate density centrifugation. The mf were then washed repeatedly in RPMI medium with antibiotics and cultured overnight at 37°C in 5% CO₂. For confocal microscopy and antigen internalization experiments, a crude saline extract of mf (21) was used. In migration experiments, the RH strain at the tachyzoite stage from the intracellular parasite *Toxoplasma gondii* was also used.

Sorting of monocytes into subsets. Monocytes from leukopacks were washed with fluorescence-activated cell sorting (FACS) medium (i.e., Hanks balanced salt solution [HBSS]) without phenol red or Ca²⁺/Mg²⁺ (BioWhittaker, Walkersville, MD) containing 1% human serum albumin (Sigma, St. Louis, MO) and 0.01% sodium azide (Sigma). Cells were first incubated with human gammaglobulin (Sigma) at 10 mg/ml for 10 min at 4°C to inhibit binding of the monoclonal antibody to Fc receptor (FcR)

and were subsequently labeled with mouse anti-human CD14 APC-Cy7 (clone 61D3; BD Biosciences, San José, CA) and CD16 A Krome Orange (clone 3G8; Beckman Coulter, Brea, CA) at saturating concentrations for 30 min at 4°C. The cells were then washed twice with FACS medium and sorted on FACSAria III, 6-laser, 15-parameter, cell sorter (Becton Dickinson, Sparks, MD) into classical (CD14^{hi}/CD16^{neg}), intermediate (CD14⁺ or ^{hi}/CD16^{med}), and nonclassical (CD14⁻/CD16^{hi}) subsets by gating on monocytes and excluding the doublets.

In vitro culture of monocytes. Unsorted or sorted (see above) monocytes were cultured at 8.3 × 10⁶ cells per well of a six-well plate in serum-free medium for 2 h, after which the medium was removed, and RPMI 1640 medium (BioWhittaker) supplemented with 20 mM glutamine (BioWhittaker), 2% heat-inactivated human AB serum (Gemini Bio-Products, West Sacramento, CA), 100 IU/ml penicillin, and 100 g/ml streptomycin (Biofluids Division, BioSource International, Rockville, MD) were added. Monocytes were subsequently cultured in medium alone or in the presence of live mf (50,000 per well), recombinant human (rh)IL-4 (50 ng/ml), or a combination of LPS (1 µg/ml; InvivoGen, San Diego, CA) and IFN-γ (20 ng/ml) for 48 h. In some experiments, monocytes were cultured with 50,000 live mf separated by transwells. The number of mf was chosen to reflect physiologically relevant concentrations. After 48 h, the cells were harvested with EDTA/EDTA (Biofluids Division, BioSource International), washed twice with PBS (without Ca²⁺/Mg²⁺), counted by trypan blue exclusion, and used in functional studies.

Cytokine measurement. In all figures, CCL22 and CCL13 were measured in monocyte culture supernatants using ELISAs from R&D Systems (Minneapolis, MN). The production of IL-1α, IL-1β, IL-6, IL-10, and TNF-α in culture supernatants was measured with a Milliplex human cytokine/chemokine magnetic bead panel kit (EMD Millipore, Billerica, MA) and the Luminex 100/200 system (Luminex, Austin, TX). The lower limit of detection for these samples was 3.2 pg/ml.

Immunofluorescence and confocal microscopy. Sorted monocytes were cultured at 10⁶ per well in a six-well plate. Cells were then either exposed to 5 µg/ml of mf antigen or left unexposed for 24 h. The cells were harvested and placed onto L-polylysine-coated slides (100,000 cells/slide) by using a cytospin apparatus. The cells were then fixed with 2% paraformaldehyde prewarmed to room temperature for 20 min. Slides were washed two times with PBS and once in 1× permeabilizing buffer (2% Triton X-100), followed by blocking for 30 min at 4°C in blocking buffer with 3% bovine serum albumin and 5% goat serum. Monocytes were then incubated overnight at 4°C in either 1:100 rabbit prebleed sera (control) or 1:100 rabbit polyclonal anti-*B. malayi* antibody (both antibodies were prepared by NIAID core facility). The cells were washed three times with permeabilizing buffer and exposed to Alexa Fluor 568-conjugated goat anti-rabbit immunoglobulin G (Invitrogen, San Diego, CA) at a concentration of 10 µg/ml for 1 h at 4°C. After three washes with PBS, cell nuclei were stained with DAPI (4',6'-diamidino-2-phenylindole) at a final con-

centration of 2 $\mu\text{g/ml}$, followed by three additional washes. Slide covers were mounted using Mowiol mounting reagent (Calbiochem, San Diego, CA). Confocal images were collected using a Leica DMI 6000 confocal microscope (Leica Microsystems, Exton, PA) enabled with a $\times 63$ oil immersion objective NA 1.4 lens. Images were acquired by using constant laser intensity and photomultiplier electronic gain to quantify the differences in absolute intensity levels upon mf antigen uptake. Images were further analyzed using Imaris image processing software (Bitplane USA, South Windsor, CT) and ImageJ imaging software (public domain, open source [NIH]) for the total intensity of images after exposure to mf antigens. Cumulative intensity calculated from 10 cells was averaged and plotted as the mean average intensity. The quantification was carried out for at least 10 fields for each condition (an average of 40 to 45 cells). The experiment was done in three independent donors.

Migration assay. Human umbilical vein endothelial cells (HUVECs; Lonza, Walkersville, MD) were cultured in EGM-2MV medium (Lonza) in T75 tissue culture flasks, harvested, and then plated in 24-well transwells (3.0 μM ; Greiner Bio-One, Monroe, NC) at a density of 0.2×10^6 cells per insert in regular 24-well tissue culture plates. HUVECs were grown until becoming a confluent monolayer for 48 h in EMG-2MV medium. The medium was aspirated, and the inserts were gently washed twice with HBSS by incubating them for 1 h. The 24-well transwell inserts were transferred to 24-well black Visiplates with clear bottoms (Perkin-Elmer NEN, Boston, MA) to minimize the background fluorescence. Monocyte populations were labeled with the nonspecific fluorescent stain PKH67 (Sigma-Aldrich) according to the manufacturer's instructions. The fluorescence-stained monocyte populations or unstained control cells were gently added into individual transwell inserts with or without live mf (5,000 mf/insert) or the RH strain of the tachyzoite stage from the intracellular parasite *T. gondii* (at a ratio of 1:5 [tachyzoites to cells]), followed by incubation at 37°C. Fluorescence emission of the migrated cells in the lower compartment was measured after 2 h using a Victor V multilabel counter (Perkin-Elmer). The data are expressed as relative fluorescence units.

T cell culture and analysis by flow cytometry. mf-unexposed or exposed monocytes were harvested and cultured with carboxyfluorescein diacetate succinimidyl ester (CFSE; Molecular Probes, Eugene, OR)-labeled autologous lymphocytes (at a 1:2 monocyte/T cell ratio with 0.5×10^6 monocytes and 1×10^6 T cells per well) either in medium alone or with 10 $\mu\text{g/ml}$ anti-CD3 in 24-well tissue culture plates (Costar, Cambridge, MA). After 4 days of culture, CFSE-labeled lymphocytes were harvested, and the proliferation of CD4^+ and CD8^+ T cells was measured by flow cytometry using a combination of antigen-presenting cell-conjugated anti-CD4 and Alexa Fluor 700 (Life Technologies, Gaithersburg, MD)-conjugated anti-CD8. The cells were then analyzed by acquisition of 50,000 events/tube using a BD FACSCanto II (BD Biosciences). Compensation was performed in every experiment using BD CompBeads (BD Bioscience) for single-color controls and unstained cells. Nonviable cells and granulocytes were excluded from analysis based on forward and side scatter. CFSE-labeled lymphocytes were further gated on expression of CD4 or CD8, and proliferation was measured in the fluorescein isothiocyanate channel for the dilution of CFSE. Proliferation indices were calculated by using the FlowJo proliferation analysis program (Tree Star, Ashland, OR).

Flow cytometry analysis for monocyte subsets in human subjects. Cells from whole blood were labeled with anti-CD14 and anti-CD16 as described above. Acquisition was accomplished on the FACSCanto II (BD Biosciences) with standard configuration, and analysis of monocyte subsets was performed using FlowJo software v9.4.10. Monocytes were gated on the nonlymphocyte population, and the CD16^+ HLA-DR^- population was excluded. Monocytes were classified as described above into classical, intermediate, and nonclassical subsets based on CD14 and CD16 staining. The frequency of each subset was calculated as the percentage of all monocytes (after the exclusion of CD16^+ HLA-DR^- cells).

Statistical analysis. Unless noted otherwise, geometric means (GM) were used as a measure for central tendency. The nonparametric Wilcoxon signed-rank test was used for paired data comparisons; for unpaired statistical analysis, the Mann-Whitney U test was used. All analyses were performed using GraphPad Prism 5.0 (GraphPad Software, Inc., San Diego, CA). All *P* values were corrected for multiple comparisons using the Holm correction with the R statistics package.

RESULTS

Nonclassical monocytes produce the lowest basal cytokine levels. To characterize the function of each of the monocyte subsets and to understand the relationship between these subsets and alternative activation, we obtained elutriated monocytes from healthy blood bank volunteers and sorted these cells by flow cytometry based on CD14 and CD16 staining to obtain highly purified classical ($\text{CD14}^{\text{hi}}/\text{CD16}^-$), intermediate ($\text{CD14}^+/\text{CD16}^{\text{med}}$), and nonclassical ($\text{CD14}^-/\text{CD16}^{\text{hi}}$) monocyte subsets (Fig. 1A). As expected, the classical monocytes made up the majority of the total monocytes—about 85 to 95%, with the intermediate and nonclassical monocytes ranging anywhere from 1.5 to 8% of the cells depending on the donors sorted (Fig. 1A, and data not shown), with findings very similar to those of other published prior studies (1, 18). After sorting, we assessed the ability of the three subsets to produce and secrete cytokines that have been used to define inflammatory (TNF- α), regulatory (IL-10), or alternative activation (CCL22) in human cells (Fig. 1B and C). In the absence of exogenous stimulation, the classical and intermediate populations produced the highest per cell levels of TNF- α , IL-10, and CCL22 and significantly more than those of the nonclassical monocytes (Fig. 1C, *P* = 0.01). Similar results were observed when IL-1 α , IL-1 β , or IL-6 were measured (data not shown).

The nonclassical subset of monocytes produced the smallest amount of cytokines in response to stimulation. To assess the ability of the different monocyte subsets to respond to exogenous stimulation known to polarize monocytes *in vitro*, we exposed the sorted monocyte subsets to LPS/IFN- γ or IL-4 and assessed the production of TNF- α , IL-10, and CCL22. Although the combination of LPS/IFN- γ induced CCL22 in the classical subset (Fig. 2B), it did stimulate production of proinflammatory cytokines in all three monocyte populations—with significantly lower production, however, in the nonclassical subset (*P* < 0.01; Fig. 2A). Similarly, production of IL-10 was induced equally in both classical and intermediate populations but was absent in the nonclassical subset (Fig. 2A). As expected, stimulation with IL-4 did not result in production of any of the inflammatory cytokines (Fig. 2B for TNF- α and data not shown for IL-6 and IL-1 α) nor IL-10 (Fig. 2B). The production of CCL22 (Fig. 2B) and CCL13 (data not shown), chemokines associated with alternative activation in human monocytes were also primarily induced in the classical and intermediate subset, suggesting that only the nonclassical subset has a diminished capacity of being polarized.

Monocyte subsets have differential migratory ability. Migration of monocytes across endothelial barriers is an important process in response to inflammation in the tissue (22). Because it has been shown that human nonclassical monocytes exhibit crawling activity on endothelium when adoptively transferred into mice and that this population appears to be more mobile than the classical subset (23), we assessed differences among the three human monocyte populations in their ability to migrate transendothelially. Without stimulation (media alone), the intermediate popu-

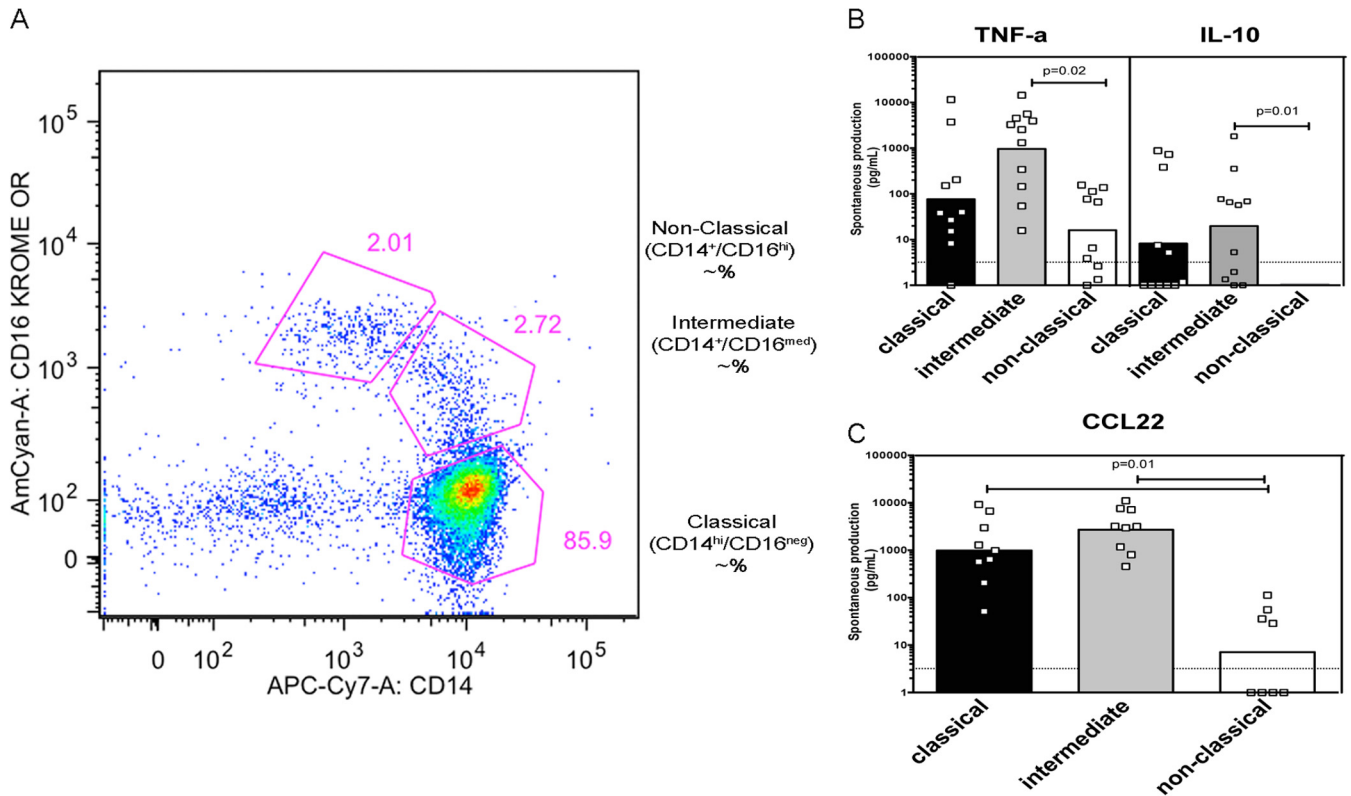


FIG 1 Nonclassical monocytes produce the lowest basal cytokine levels. (A) Flow cytometry dot plot showing gating strategy of the three monocyte subsets based on the expression of CD14 and CD16. Monocyte subsets are indicated as classical, intermediate, and nonclassical. Spontaneous production of cytokines (TNF- α and IL-10 [B] and CCL22 [C]) was measured in 48-h culture supernatants in classical (closed bars [■]), intermediate (gray bars [▒]), and nonclassical (open bars [□]) monocyte subsets. Supernatants were evaluated for the levels of TNF- α and IL-10 by using Luminex and CCL22 by using ELISA. Bars are expressed as the geometric mean of spontaneous production in 8 to 11 independent donors. Each dot represents an independent donor. A paired *t* test and a nonparametric Wilcoxon signed-rank test were used for comparisons between groups.

lation was shown to migrate least well across an endothelial barrier compared to the other two monocyte subsets (Fig. 3; *P* = 0.03).

Classical monocytes are better able to promote proliferation of both CD4⁺ and CD8⁺ T cells. To assess whether the three

monocyte subsets promote T cell proliferation differentially, each subset was cocultured with CFSE-labeled autologous lymphocytes in the presence of soluble anti-CD3, and proliferation was measured (Fig. 4). As can be seen, monocytes from the classical pop-

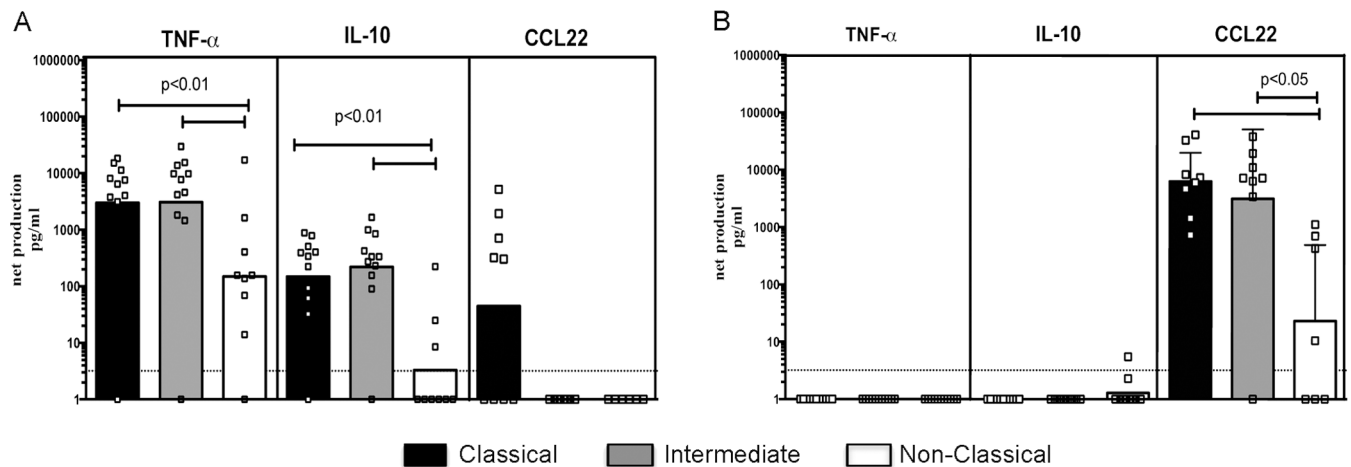


FIG 2 Human monocytes subsets are polarized differentially. Monocyte subsets—classical (closed bars [■]), intermediate (gray bars [▒]), and nonclassical (open bars [□])—were cultured with LPS at 1 μ g/ml and IFN- γ at 10 ng/ml (A) and IL-4 at 10 ng/ml (B) for 48 h. The supernatants were collected and evaluated for the levels of TNF- α and IL-10 by using Luminex and CCL22 by using ELISA. The data are expressed as the geometric mean (A) and geometric mean with 95% CI (B) of net production (media subtracted) in 6 to 11 donors in panel A and in 7 to 11 donors in panel B. Each dot represents an independent donor. A paired *t* test and a nonparametric Wilcoxon signed-rank test were used for comparisons between groups.

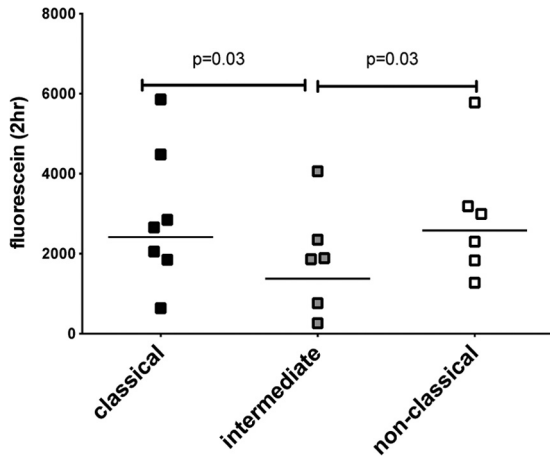


FIG 3 Intermediate monocytes have the lowest ability in transendothelial migration. Transendothelial migration of PKH67-labeled-monocyte subsets through confluent monolayers of HUVECs was measured in HBSS (media) alone. Fluorescence emission of the migrated cells in the lower compartment was measured after 2 h. The data are expressed as the geometric mean of net (unlabeled subtracted) relative fluorescence units from four to five independent donors. Each dot represents an independent donor. A paired *t* test and a nonparametric Wilcoxon signed-rank test were used for comparisons between groups.

ulation promoted both CD4⁺ (stimulation index [SI] = 2.04) and CD8⁺ (SI = 2.04) T cell proliferation (Fig. 4) to a greater degree than did either the nonclassical (SI = 1.75 for CD4⁺ and 1.71 for CD8⁺) or the intermediate (SI = 1.76 for CD4⁺ and 1.72 for CD8⁺) monocytes.

Filaria-infected individuals exhibit significantly elevated frequencies and absolute numbers of circulating nonclassical monocytes. Although expansion of particular monocyte subsets as a consequence of bacterial and viral infection has been demonstrated (1), their distribution in human helminth infections remains unstudied. Therefore, we first measured *ex vivo* frequencies and absolute numbers of classical, intermediate, and nonclassical monocytes in filaria-infected (INF; *n* = 11) and uninfected healthy (UN; *n* = 13) individuals (Table 1) using a whole-blood staining strategy (see Fig. S1 in the supplemental material). As can be seen in Fig. 5, the *ex vivo* frequency of classical monocytes in INF individuals was significantly lower than the frequencies in UN individuals (INF GM = 35.6% versus UN GM = 51.3%; *P* < 0.0001), as was the frequency of intermediate monocytes (INF GM = 1.5% versus UN GM = 2.3%; *P* < 0.0001) (Fig. 5). Interestingly, the *ex vivo* frequency and absolute numbers of monocytes demonstrated a significantly higher number (*P* < 0.0001) of the

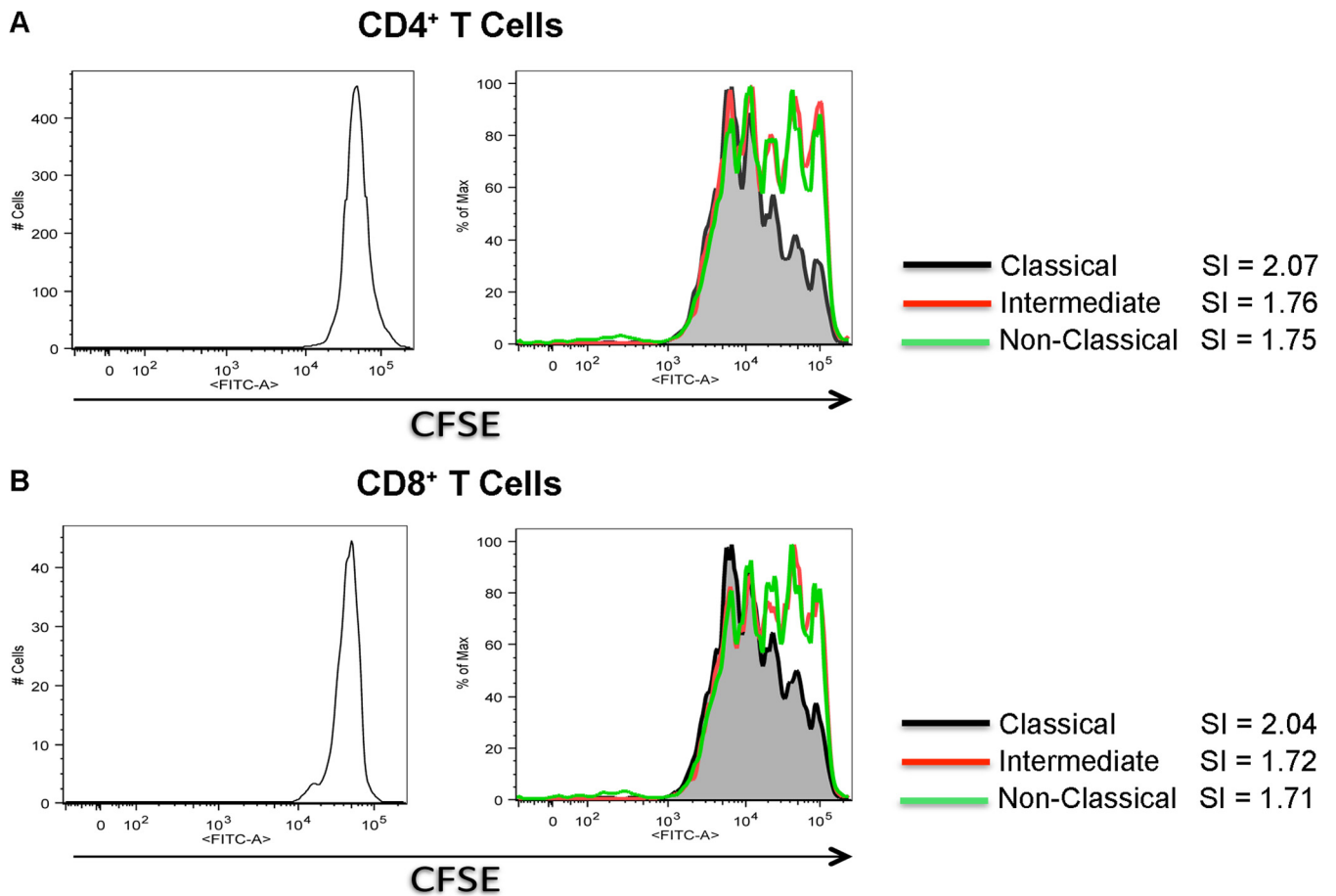


FIG 4 Classical monocytes are better able to promote anti-CD3-dependent proliferation of CD4⁺ and CD8⁺ T cells. Classical (shaded areas), intermediate (red lines), and nonclassical (green lines) monocytes were cocultured with CFSE-labeled autologous lymphocytes (1:2 ratio, monocytes to lymphocytes) in the presence of 10 μg of soluble anti-CD3/ml for 4 days. Flow cytometry was performed, and the cells were gated based on CD4 or CD8 expression. Representative data are shown for the CFSE expression of each population in one donor (total tested, 4 to 5). The stimulation index (SI) is shown for each monocyte population for CD4⁺ (A) and CD8⁺ (B) cells. The left panels represent control conditions with no T cell proliferation in the absence of anti-CD3.

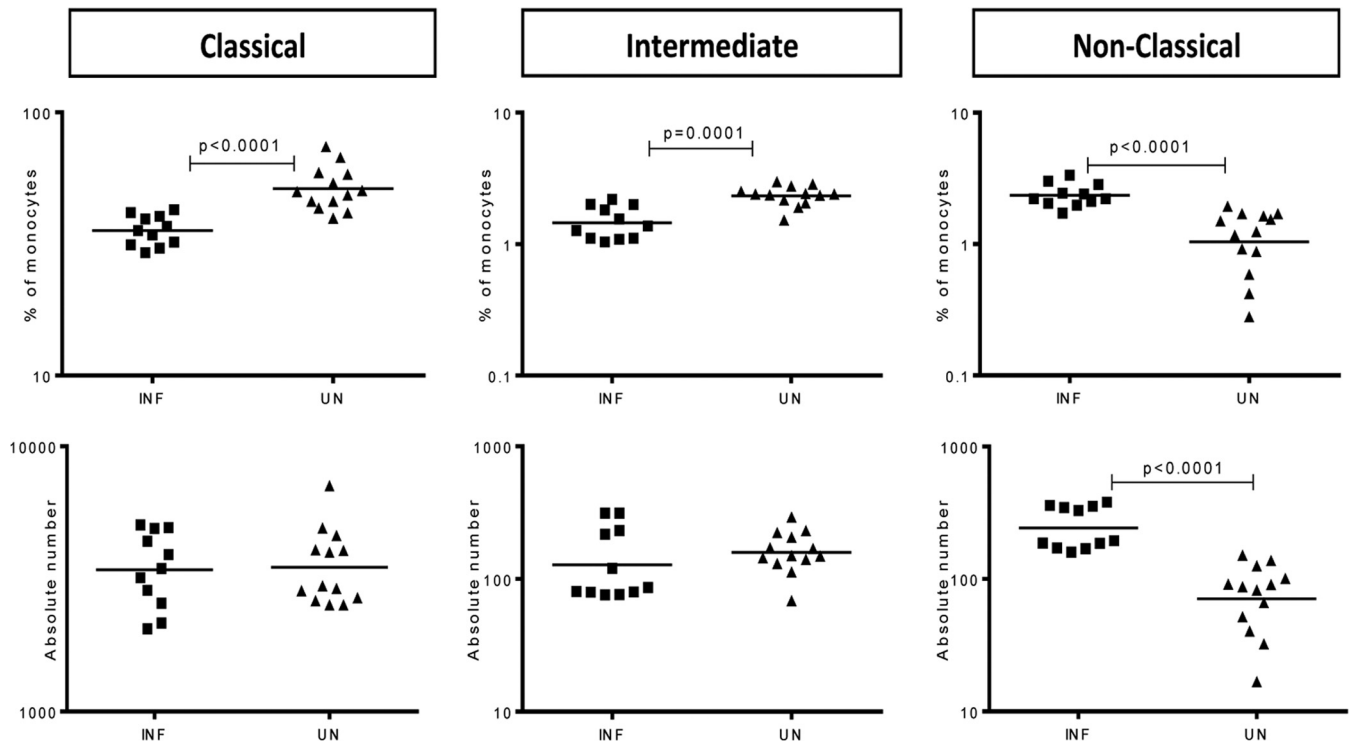


FIG 5 Filaria-infected (INF) individuals exhibit significantly increased frequencies and absolute numbers of circulating nonclassical monocytes. Cells from whole blood were labeled with anti-CD14 and anti-CD16. Monocytes were gated on the nonlymphocyte population, and the CD16⁺ HLA-DR⁻ population was excluded. Monocytes were classified as classical, intermediate, and nonclassical on the basis of CD16 and CD14 expression in whole blood. The frequencies (top row) and absolute numbers (bottom row) of classical, intermediate, and nonclassical monocytes were measured *ex vivo* by flow cytometry and by using differential hematology counts in INF individuals ($n = 11$) and in UN individuals ($n = 13$). The data are shown as scatter plots, with each symbol representing a single individual. P values were calculated by using the Mann-Whitney U test.

nonclassical subset in INF individuals (GM = 2.4%; GM = 243; range, 381 to 159.) compared to UN individuals (GM = 1.04%; GM = 71; range, 17 to 151). Together, these data indicate that filarial infection (associated with the presence of circulating parasite antigen) is linked with significant perturbations in the distribution and number of circulating monocyte subsets.

Monocyte subsets have a differential ability to internalize soluble parasite antigen. Having identified the filaria-induced alterations in monocyte subset distributions and shown that each of the monocyte subsets serve some distinct functions in healthy individuals, we assessed the ability of these three distinct monocyte subsets to internalize parasite antigen. As can be seen, the classical monocyte population internalized mf antigen to a much greater extent than did the intermediate subset both qualitatively (Fig. 6A) and quantitatively (Fig. 6B); the nonclassical monocytes internalized little to no antigen.

Differential regulation of monocyte subsets to live mf of *B. malayi*. To understand better the interaction between the circulating parasites seen in filarial infection and their influence on each of the three monocyte subsets, we exposed each of the subsets to live microfilariae. Although cytokine production was induced by mf to some degree in each of the three subsets, IL-10 was induced by these parasites primarily in the intermediate subset (Fig. 7A). Moreover, mf altered transendothelial migration quite dramatically in the nonclassical population ($P = 0.03$ compared to unexposed monocytes), a process that appears to be filarial parasite specific since the response to an intracellular parasite, *T. gondii*, failed to inhibit monocyte migration (Fig. 7B).

DISCUSSION

Although the discovery of different human monocyte subsets has shed light on qualitative differences among these cells, it is still not clear whether each of these monocyte subserves a unique function. Monocytes and macrophages have recently been separated not only by their phenotype but also by differences in function. Many previous studies have indicated that M1 macrophages and the cytokines they produce are important in host defense against intracellular pathogens but that they also contribute to immune-mediated pathology. In contrast, M2 macrophages have been identified with phenotypes distinct from M1 and have a broad range of activities, including wound repair (12). A third group of macrophages, Mreg (14), has also been identified. These macrophages—often generated by stimulation with high-density immune complexes—have been shown to produce a significant amount of IL-10 (13).

While different gating strategies may reveal different phenotypes and more than three subsets of monocytes (17), in the present study, we sorted human monocytes—based on expression of CD14 and CD16—into three subpopulations: classical (CD14^{hi}/CD16^{neg}), intermediate (CD14^{+/hi}/CD16^{med}), and nonclassical (CD14⁺/CD16^{hi}) (Fig. 1A). At baseline, a conspicuous difference among the three monocyte subsets was the heterogeneous nature of the cytokines produced. This feature was particularly prominent in the nonclassical population, which had the lowest levels of spontaneous production of all cytokines measured, including the proinflammatory cytokine (TNF- α), chemokine associated with

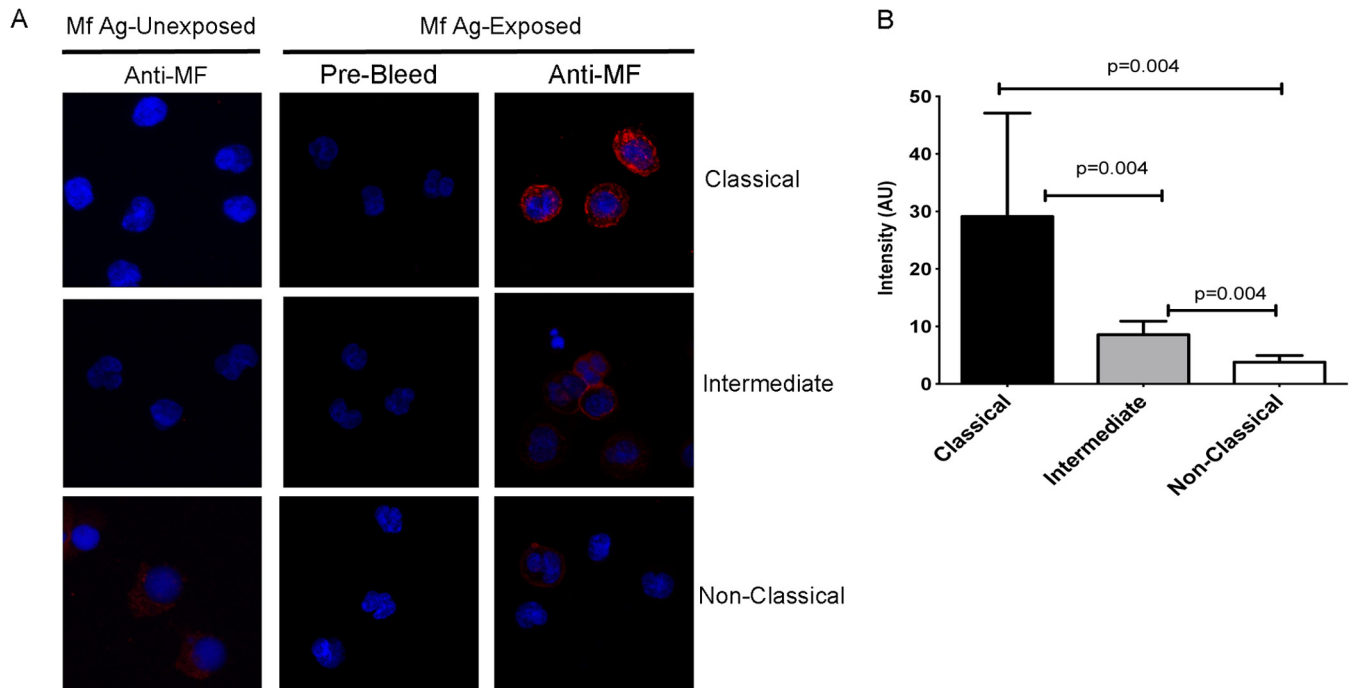


FIG 6 Classical monocytes have a greater ability to internalize soluble microfilaria (mf) antigens. Monocyte subsets were either exposed to mf antigen (Mf Ag-Exposed) or left unexposed (Mf Ag-Unexposed) for 24 h. (A) Confocal microscopy (objective, $\times 63$) of monocyte subsets using either anti-mf rabbit polyclonal antibody or a negative-control antibody (polyclonal rabbit [prebleed]). (B) Cumulative average of fluorescence intensity measured in each subset represent levels of mf antigen uptake. Cumulative intensities calculated from 10 cells were averaged and plotted and are shown as the geometric mean intensity with 95% CI. A paired *t* test and a nonparametric Wilcoxon signed-rank test were used for comparisons between groups. The data represent one of three independent donors in three independent experiments.

alternative activation (CCL22), and the regulatory cytokine IL-10 (Fig. 1B and C).

Although these monocyte phenotypes have been described primarily in murine systems, a growing body of evidence has shown that these phenotypes exist in humans. In fact, human monocytes can be activated using either LPS/IFN- γ or IL-4/IL-13 to promote development of M1- or M2-type cells, respectively (16, 24–26). While M1 macrophages produce an array of inflammatory cytokines, including IL-1 α , IL-1 β , TNF- α , and IL-6, M2 macrophages in humans can be distinguished by their production of a set of chemokines, including CCL13, CCL18, and CCL22 (12, 26). In addition, stimuli such as TLR ligands and immune complexes have been identified as a requirement to generate macrophages that produce high levels of IL-10 and little IL-12 (12, 14).

Circulating human monocytes are a heterogeneous population of cells and have differential abilities to produce cytokines at homeostasis. At the basal level, nonclassical monocytes produce the lowest levels of cytokines. Furthermore, monocyte response to activation largely affects cytokine production in the classical and intermediate populations. In fact, our data show that both classical and intermediate subsets of monocytes can exhibit either an M1 (after stimulation with LPS/IFN- γ) or M2 (after stimulation with IL-4) phenotype, while the nonclassical subset appears to have little ability to differentiate into either M1 or M2 stimulation (Fig. 2). Moreover, since it has already been shown that human CD14^{dim} monocytes exhibit crawling behavior on murine endothelium when intravenously transferred to animals (5) and that CD16⁺ monocytes are far more mobile than their CD16^{neg} counterparts (23), we could show that CD16^{med} cells had a diminished

capacity to migrate transendothelially (Fig. 3). Since it has been shown that genes associated with cytoskeletal mobility are highly expressed in the nonclassical population of monocytes (6, 7), our finding that this subset has the highest cell surface expression of CD31 (the ligand for $\alpha 5\beta 3$ integrin; data not shown) suggests that the increased expression of genes associated with cytoskeletal mobility and CD31 may be responsible for the increased ability of the nonclassical monocyte subset to migrate.

The ability to internalize and present antigen is a crucial function for monocytes. Previous studies have indicated that the intermediate subset expresses high levels of major histocompatibility complex class II (6, 7), as well as the costimulatory molecules CD40 and CD54 (6), suggesting a greater ability of this subset to promote T cell proliferation. The majority of studies that measure T cell proliferation, however, have been in systems bypassing the need for antigen, using superantigens or anti-CD3. The data from the present study suggest that it is actually the classical subset (which represents the majority of circulating human monocytes) that is the most efficient at internalizing soluble parasite antigens (Fig. 6) and that this translates into better induction of CD4⁺ and CD8⁺ proliferation (Fig. 4), a finding that has been seen previously for superantigen-driven activation (7).

Expansion of CD16⁺ (intermediate and nonclassical) monocytes has been described in many different types of disorders, including bacterial and viral infections (reviewed by Wong et al. [1]). The intermediate subset, in particular, is often referred to as “proinflammatory” due to the ability of these cells to produce high levels of TNF- α and IL-6 (27, 28); however, the importance of expansion of these subsets and its relationship to the severity of

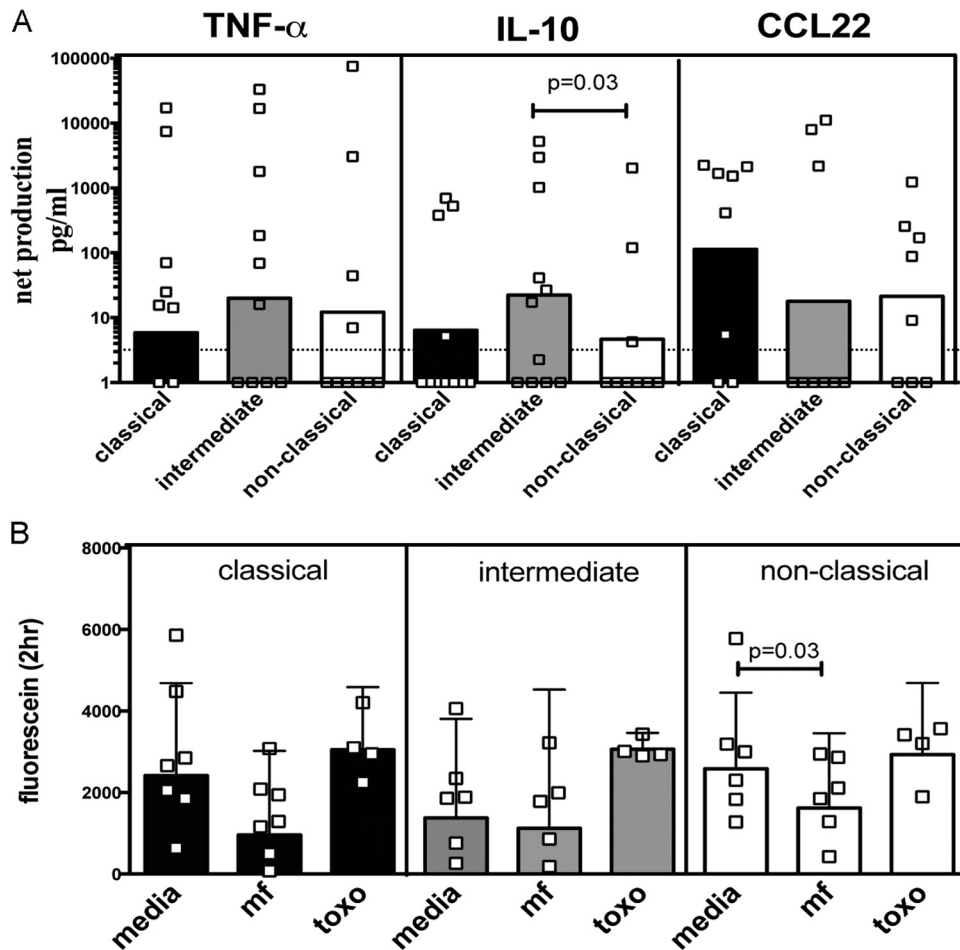


FIG 7 Human monocyte subsets exhibit differential response to live mf. (A and B) Monocyte subsets—classical (closed bars [■]), intermediate (gray bars [▒]), and nonclassical (open bars [□])—were cultured with live mf of *B. malayi* for 48 h. (A) Supernatants were collected and evaluated for the levels of TNF- α and IL-10 by using Luminex and CCL22 by using ELISA. The data are expressed as geometric mean with 95% CI net production (media subtracted) in 6 to 11 donors. Each dot represents an independent donor. (B) The transendothelial migration of PKH67-labeled-monocyte subsets through confluent monolayers of HUVECs was measured in HBSS (media) alone or in the presence of either live microfilariae of *B. malayi* ($n = 5,000$) or tachyzoites of *T. gondii* (1:5, *Toxoplasma* parasites to cells). Fluorescence emission of the migrated cells in the lower compartment was measured after 2 h. The data are expressed as the geometric mean (A) and geometric mean with 95% CI (B) of net (unlabeled subtracted) relative fluorescence units from four to five independent donors. Each dot represents an independent donor. A paired *t* test and a nonparametric Wilcoxon signed-rank test were used for comparisons between groups.

disease has not been fully elucidated. In the context of infection, the proportions of monocyte subsets have been shown to depend on ethnicity and exposure to helminth infection (17). In support of this concept, we were able to demonstrate significantly increased numbers and frequencies of particular monocyte subsets in patent filarial infection.

Having identified the filaria-induced alterations in monocyte subset distributions and having shown that each of the monocyte subsets exhibits somewhat distinct functions, we were able to model this interaction *in vitro* and show that the parasite differentially affects each of the monocyte subsets at the level of activation-induced cytokine production, T cell activation, and transendothelial migration.

Together, our data suggest that while there is plasticity among the three different subsets of human monocytes, each subpopulation may play a distinct role under normal conditions and during infection with a tissue-invasive helminth infection. Most notably, since IL-10 appears to be the major regulatory cytokine in filarial

(and other longstanding, chronic helminth) infection, the finding that monocyte-derived IL-10 may be driven by a particular parasite stage on a particular monocyte subset provides new insight into the role played by these innate circulating cells in modulating the adaptive immune response that is characteristic of many systemic helminth infections.

ACKNOWLEDGMENTS

This study was supported by the Intramural Research Program of the Division of Intramural Research, NIAID, NIH.

We thank Cathy Steel for critical reading of the manuscript and Simon Metenou and Joseph Kubofcik for technical advice and help. We thank Alan Sher, Dragana Jankovic, and Kevin Tosh for providing *Toxoplasma gondii* and Brenda Rae Marshall, DPSS, NIAID, for editing.

REFERENCES

1. Wong KL, Yeap WH, Tai JJ, Ong SM, Dang TM, Wong SC. 2012. The three human monocyte subsets: implications for health and disease. *Immunol. Res.* 53:41–57. <http://dx.doi.org/10.1007/s12026-012-8297-3>.

2. Mobley JL, Leininger M, Madore S, Baginski TJ, Renkiewicz R. 2007. Genetic evidence of a functional monocyte dichotomy. *Inflammation* 30: 189–197. <http://dx.doi.org/10.1007/s10753-007-9036-0>.
3. Ancuta P, Liu KY, Misra V, Wacleche VS, Gosselin A, Zhou X, Gabuzda D. 2009. Transcriptional profiling reveals developmental relationship and distinct biological functions of CD16⁺ and CD16⁻ monocyte subsets. *BMC Genomics* 10:403. <http://dx.doi.org/10.1186/1471-2164-10-403>.
4. Zhao C, Zhang H, Wong WC, Sem X, Han H, Ong SM, Tan YC, Yeap WH, Gan CS, Ng KQ, Koh MB, Kourilsky P, Sze SK, Wong SC. 2009. Identification of novel functional differences in monocyte subsets using proteomic and transcriptomic methods. *J. Proteome Res.* 8:4028–4038. <http://dx.doi.org/10.1021/pr900364p>.
5. Cros J, Cagnard N, Woillard K, Patey N, Zhang SY, Senechal B, Puel A, Biswas SK, Moshous D, Picard C, Jais JP, D'Cruz D, Casanova JL, Trouillet C, Geissmann F. 2010. Human CD14^{dim} monocytes patrol and sense Nucleic acids and viruses via TLR7 and TLR8 receptors. *Immunity* 33:375–386. <http://dx.doi.org/10.1016/j.immuni.2010.08.012>.
6. Wong KL, Tai JJ, Wong WC, Han H, Sem X, Yeap WH, Kourilsky P, Wong SC. 2011. Gene expression profiling reveals the defining features of the classical, intermediate, and nonclassical human monocyte subsets. *Blood* 118:e16–31. <http://dx.doi.org/10.1182/blood-2010-12-326355>.
7. Zawada AM, Rogacev KS, Rotter B, Winter P, Marel RR, Fliser D, Heine GH. 2011. SuperSAGE evidence for CD14⁺⁺ CD16⁺ monocytes as a third monocyte subset. *Blood* 118:e50–61. <http://dx.doi.org/10.1182/blood-2011-01-326827>.
8. Rossol M, Kraus S, Pierer M, Baerwald C, Wagner U. 2012. The CD14^{bright} CD16⁺ monocyte subset is expanded in rheumatoid arthritis and promotes expansion of the Th17 cell population. *Arthritis Rheum.* 64:671–677. <http://dx.doi.org/10.1002/art.33418>.
9. Grage-Griebenow E, Flad HD, Ernst M. 2001. Heterogeneity of human peripheral blood monocyte subsets. *J. Leukoc. Biol.* 69:11–20.
10. Skrzeczynska-Moncznik J, Bzowska M, Loseke S, Grage-Griebenow E, Zembala M, Pryjma J. 2008. Peripheral blood CD14^{high} CD16⁺ monocytes are main producers of IL-10. *Scand. J. Immunol.* 67:152–159. <http://dx.doi.org/10.1111/j.1365-3083.2007.02051.x>.
11. Smedman C, Ernemar T, Gudmundsdotter L, Gille-Johnson P, Somell A, Nihlmark K, Gärdlund B, Andersson J, Paulie S. 2011. FluoroSpot analysis of TLR-activated monocytes reveals several distinct cytokine secreting subpopulations. *Scand. J. Immunol.* 75:249–258. <http://dx.doi.org/10.1111/j.1365-3083.2011.02641.x>.
12. Mosser DM, Edwards JP. 2008. Exploring the full spectrum of macrophage activation. *Nat. Rev. Immunol.* 8:958–969. <http://dx.doi.org/10.1038/nri2448>.
13. Sutterwala FS, Noel GJ, Salgame P, Mosser DM. 1998. Reversal of proinflammatory responses by ligating the macrophage Fcγ receptor type I. *J. Exp. Med.* 188:217–222. <http://dx.doi.org/10.1084/jem.188.1.217>.
14. Anderson CF, Mosser DM. 2002. A novel phenotype for an activated macrophage: the type 2 activated macrophage. *J. Leukoc. Biol.* 72:101–106.
15. Fleming BD, Mosser DM. 2011. Regulatory macrophages: setting the threshold for therapy. *Eur. J. Immunol.* 41:2498–2502. <http://dx.doi.org/10.1002/eji.201141717>.
16. Semnani RT, Mahapatra L, Moore V, Sanprasert V, Nutman TB. 2011. Functional and phenotypic characteristics of alternative activation induced in human monocytes by interleukin-4 or the parasitic nematode *Brugia malayi*. *Infect. Immun.* 79:3957–3965. <http://dx.doi.org/10.1128/IAI.05191-11>.
17. Appleby LJ, Nausch N, Midzi N, Mduluzi T, Allen JE, Mutapia F. 2013. Sources of heterogeneity in human monocyte subsets. *Immunol. Lett.* 152:32–41. <http://dx.doi.org/10.1016/j.imlet.2013.03.004>.
18. Novais FO, Nguyen BT, Beiting DP, Carvalho LP, Glennie ND, Passos S, Carvalho EM, Scott P. 2014. Human classical monocytes control the intracellular stage of *Leishmania brasiliensis* by reactive oxygen species. *J. Infect. Dis.* 209:1288–1296. <http://dx.doi.org/10.1093/infdis/jiu013>.
19. Semnani RT, Keiser PB, Coulibaly YI, Keita F, Diallo AA, Traore D, Diallo DA, Doumbo OK, Traore SF, Kubofcik J, Klion AD, Nutman TB. 2006. Filaria-induced monocyte dysfunction and its reversal following treatment. *Infect. Immun.* 74:4409–4417. <http://dx.doi.org/10.1128/IAI.01106-05>.
20. Babu S, Blauvelt CP, Kumaraswami V, Nutman TB. 2005. Diminished expression and function of TLR in lymphatic filariasis: a novel mechanism of immune dysregulation. *J. Immunol.* 175:1170–1176. <http://dx.doi.org/10.4049/jimmunol.175.2.1170>.
21. Semnani RT, Sabzevari H, Iyer R, Nutman TB. 2001. Filarial antigens impair the function of human dendritic cells during differentiation. *Infect. Immun.* 69:5813–5822. <http://dx.doi.org/10.1128/IAI.69.9.5813-5822.2001>.
22. Muller WA. 2011. Mechanisms of leukocyte transendothelial migration. *Annu. Rev. Pathol.* 6:323–344. <http://dx.doi.org/10.1146/annurev-pathol-011110-130224>.
23. Randolph GJ, Sanchez-Schmitz G, Liebman RM, Schakel K. 2002. The CD16⁺ (FcγRIII⁺) subset of human monocytes preferentially becomes migratory dendritic cells in a model tissue setting. *J. Exp. Med.* 196:517–527. <http://dx.doi.org/10.1084/jem.20011608>.
24. Martinez FO, Gordon S, Locati M, Mantovani A. 2006. Transcriptional profiling of the human monocyte-to-macrophage differentiation and polarization: new molecules and patterns of gene expression. *J. Immunol.* 177:7303–7311. <http://dx.doi.org/10.4049/jimmunol.177.10.7303>.
25. Martinez FO, Helming L, Gordon S. 2009. Alternative activation of macrophages: an immunologic functional perspective. *Annu. Rev. Immunol.* 27:451–483. <http://dx.doi.org/10.1146/annurev.immunol.021908.132532>.
26. Tiemessen MM, Jagger AL, Evans HG, van Herwijnen MJ, John S, Taams LS. 2007. CD4⁺ CD25⁺ Foxp3⁺ regulatory T cells induce alternative activation of human monocytes/macrophages. *Proc. Natl. Acad. Sci. U. S. A.* 104:19446–19451. <http://dx.doi.org/10.1073/pnas.0706832104>.
27. Frankenberger M, Sternsdorf T, Pechumer H, Pforte A, Ziegler-Heitbrock HW. 1996. Differential cytokine expression in human blood monocyte subpopulations: a polymerase chain reaction analysis. *Blood* 87:373–377.
28. Belge KU, Dayyani F, Horelt A, Siedlar M, Frankenberger M, Espevik T, Ziegler-Heitbrock L. 2002. The proinflammatory CD14⁺ CD16⁺ DR⁺⁺ monocytes are a major source of TNF. *J. Immunol.* 168:3536–3542. <http://dx.doi.org/10.4049/jimmunol.168.7.3536>.